Available online at www.sciencedirect.com
SCIENCE DIRECT
Catalysis Today 110 (2005) 38–46
CATALYSIS TODAY
www.elsevier.com/locate/cattod

# Hydrothermal synthesis and characterization of ZSM-5 coatings on a molybdenum support and scale-up for application in micro reactors

M.J.M. Mies [a], J.L.P. van den Bosch [a], E.V. Rebrov [a], J.C. Jansen [b], M.H.J.M. de Croon [a], J.C. Schouten [a,*]

[a] *Department of Chemical Engineering and Chemistry, Schuit Institute of Catalysis, Eindhoven University of Technology, P.O. Box 513, 5600 MB Eindhoven, The Netherlands*
[b] *Faculty of Applied Sciences, Delft University of Technology, Julianalaan 136, 2628 BL Delft, The Netherlands*

Available online 28 October 2005

**Abstract**

A procedure has been developed to grow ZSM-5 crystals in situ on a molybdenum (Mo) support. The high heat conductivity (138 W/mK) and high mechanical stability at elevated temperatures of the Mo support allow the application of ZSM-5 coatings in micro reactors for high temperature processes involving large heat effects. The effect of the synthesis mixture composition on ZSM-5 coverage and on the uniformity of the ZSM-5 coatings was investigated on plates of $10 \times 10$ mm$^2$. Ratios of $H_2O/Si = 50$, $Si/Al = 25$, and $TPA/Al = 2.0$ were found to be optimal for the formation of uniform coatings of 6 g/m$^2$ at a temperature of 150 °C and a synthesis time of 48 h. Scaling up of the synthesis procedure on 72 Mo plates of $40 \times 9.8 \times 0.1$ mm$^3$ resulted in a uniform coverage of $14.8 \pm 0.4$ g/m$^2$. The low deviation per individual plate (<3%) indicates the uniformity of the synthesis conditions in the scale-up procedure.


*Keywords:* ZSM-5; Molybdenum; In situ zeolite synthesis; Scale-up procedure; Micro reactors

## 1. Introduction

The interest in the preparation of zeolitic films has increased enormously during the last decade due to their versatile applications as membranes [1], chemical sensors [2], and catalytic coatings [3–5]. In the latter case, both the framework and charge compensating cations can be easily substituted by other elements creating an active catalyst. Recent developments show the potential of zeolitic coatings in chemical synthesis, e.g. Fe-ZSM-5 for benzene to phenol oxidation [6], Mo-ZSM-5 for methane dehydrogenation [7], and Co-ZSM-5 for ammoxidation of ethane to acetonitrile [8,9]. Many processes can be considerably intensified by combination of the high intrinsic surface area of zeolites (400–700 m$^2$/g) with a large geometrical surface area of micro structured reactors (5000–10,000 m$^2$/m$^3$). Furthermore, implementation of zeolitic coatings in micro reactors has several advantages such as a low-pressure drop, a narrow residence time distribution, high heat and mass transfer rates, and a possibility to carry out the reaction in the explosive region [10]. Finally, micro reactors can be regarded as the natural platform for the high-throughput screening of zeolitic coatings [11].

Micro reactors are typically built up from several dozens up to several hundreds of individual reactor plates or channels on which the catalytic coating is deposited. Another important characteristic of micro structured reactors is that they are amenable to scale-out [12]. So, the production can be increased by increasing the number of reactors, and thus the number of reactor plates, rather than the size. The performance of reactors, especially micro reactors, depends on the uniformity of the catalytic coatings. A non-uniform chemical composition of the catalytic coatings as well as variations in coating thickness, which will result in a broader flow distribution [13,14], will affect the conversion and selectivity of the chemical process. Therefore, the implementation of e.g. zeolitic coatings in micro reactors requires the development of a scale-up procedure to simultaneously synthesize identical coatings on a large number of reactor plates or channels. Non-uniformities between the coatings can be avoided when all reactor plates are treated in one

* Corresponding author. Tel.: +31 40 247 2850; fax: +31 40 244 6653.
*E-mail address:* j.c.schouten@tue.nl (J.C. Schouten).
*URL:* http://www.chem.tue.nl/scr

0920-5861/$ – see front matter © 2005 Elsevier B.V. All rights reserved.
doi:10.1016/j.cattod.2005.09.015

single deposition step, e.g. a large volume of a synthesis mixture in case of the in situ growth of zeolitic coatings on a multitude of reactor plates.

Despite the opportunities of zeolitic micro reactors, this field has been scarcely explored so far [15]. Hydrothermal synthesis of zeolites on various substrate materials as metals [16–18] and ceramics [19–21] has been thoroughly investigated. Recently, we demonstrated that stable layers of ZSM-5 crystals can be in situ grown from the synthesis mixture on the surface of the channels and thin walls of a micro reactor made of AISI-316 stainless steel [22]. However, this material is not the best choice for the application in high temperature micro reactors because of the low thermal conductivity and corrosion resistance at elevated temperatures. On the contrary, refractory metals have high melting points, an improved corrosion resistance [23], and low thermal expansion coefficients. Furthermore, some of them (e.g. molybdenum) have a high heat conductivity. Therefore, the application of zeolitic coatings in micro structured reactors made in refractory metals [11,24] requires the development of a synthesis procedure on these advanced materials.

In our previous work, we presented the design of a molybdenum high throughput micro reactor (HTMR) for the screening of catalytic coatings [11]. This reactor can be used especially in high temperature gas phase reactions involving large heat effects. The ammoxidation of light paraffins over cobalt exchanged ZSM-5 zeolites is an example of such a process [8,9]. In this paper, a procedure is developed for the hydrothermal synthesis of ZSM-5 coatings on molybdenum plates of 10 × 10 $mm^2$. The synthesis parameters have been optimized in order to obtain coatings with a zeolite coverage between 2 and 15 $g/m^2$, where the latter value corresponds with an average thickness of the coating of 12 μm. The lower limit corresponds to a single layer of zeolite crystals [22], while the upper limit is set due to the physical dimensions of the microstructures in the walls of the HTMR (130 μm) and the thickness of the molybdenum plates (100 μm). The design of the reactor requires a multitude of identical sets of eight coatings of 40 × 9.8 $mm^2$. These coatings can be loaded with a series of active species of various contents in separate ion exchange procedures in order to optimize the zeolitic coating activity and selectivity. Therefore, a scale-up procedure is developed to simultaneously synthesize ZSM-5 coatings on 72 molybdenum reactor plates. In the following we describe the synthesis and characterization of ZSM-5 coatings on a molybdenum support and the scale-up of the synthesis procedure.

## 2. Experimental

### 2.1. Materials

Molybdenum foil (Aldrich, 99.9+%) of 100 μm in thickness was cut in plates of 10 × 10 $mm^2$ and 40.0 × 9.8 $mm^2$ for experiments for the optimization of the ZSM-5 synthesis procedure and for the development of the scale-up procedure, respectively. In this study experiments for the optimization of ZSM-5 synthesis were conducted on molybdenum (Mo) as well as on surface modified Titania–Alumina–Molybdenum (TAMo). The pretreatment procedures for both plates are summarized in Table 1.

Mo plates were pretreated according to steps 1 to 4 of Table 1. Steps 1 to 3 are cleaning and etching steps according to a procedure described in [17]. Before synthesis, the Mo plate was dipped in a solution of the templating agent (step 4), and then dried for 1 h at 110 °C.

TAMo plates were obtained after deposition of thin layers of $Al_2O_3$ and $TiO_2$ (steps 5 and 6, respectively) on an etched surface of molybdenum (after steps 1 and 2) by atomic layer deposition (ALD). Molybdenum plates were cleaned in a concentrated HCl solution prior to the ALD process. The $Al_2O_3$ film was deposited on the Mo surface by ALD with TMA (trimethylaluminium) as the metal precursor and $H_2O$ as oxidation precursor at a temperature of 250 °C. The growth of the $TiO_2$ film on the $Al_2O_3$ film was performed from $TiCl_4$ (titaniumchloride) and $H_2O$ sources at 500 °C. Every precursor pulse in the tubular glass ALD reactor was alternated with an inert argon pulse. The $Al_2O_3$ film has to protect the molybdenum plate from oxidation at reaction conditions while the $TiO_2$ film can be made hydrophilic by UV irradiation. TAMo plates were treated by UV radiation with wavelengths in the range of 220–1400 nm for 3 h (Hanovia 679A-36 equipment, 450 W) prior to the zeolite synthesis procedure.

### 2.2. Small scale synthesis of zeolitic coatings

The synthesis mixtures were prepared by adding tetraethylorthosilicate (TEOS, >98%, Merck) as the silica source to a mixture of sodium aluminate ($NaAlO_2$, 95%, technical grade, Riedel de Haën) as the alumina source, tetrapropylammonium hydroxide (TPAOH, 40 wt.%, Merck) as the template agent, and demineralized water. In this study the synthesis mixtures were prepared within the following composition range: (32–100)$SiO_2$:1$Al_2O_3$:(4.0–11)TPAOH:(960–10.000)$H_2O$. Before the synthesis, the solution was hydrolyzed for 23 h at 47 °C under continuous stirring. Then, demineralized water was added to the synthesis mixture to compensate for the extra weight loss of water after the aging procedure. The plates were

Table 1
Pretreatment procedures of molybdenum (Mo) and Titania–Alumina–Molybdenum (TAMo) plates[a]

| Sequence | Procedure | Conditions | Plates | |
|---|---|---|---|---|
| | | | Mo | TAMo |
| 1 | Xylene | 140 °C, 1 h | + | + |
| 2 | $NH_4OH/H_2O_2/5H_2O$[b,c] | 80 °C, 45 s | + | + |
| 3 | $HCl/H_2O_2/6H_2O$[d] | 80 °C, 45 s | + | – |
| 4 | 10 wt.% TPAOH[e] | 25 °C, 60 s | + | – |
| 5 | ALD of 170 nm $Al_2O_3$ | 250 °C | – | + |
| 6 | ALD of 50 nm $TiO_2$ | 500 °C | – | + |

ALD denotes atomic layer deposition, which was performed at Nanoscale Oy, Finland (http://www.nanoscale.fi/).

[a] Dimension of plates: 11 × 9.8 × 0.1 $mm^3$ and 40 × 9.8 × 0.1 $mm^3$.

[b] Riedel de Haën (25 wt.%).

[c] Fluka (30 wt.%).

[d] Aldrich (37 wt.%).

[e] Merck (20 wt.%).

positioned on a polyetheretherketone (PEEK) holder parallel to the axis of the autoclave at 1 cm below the gas–liquid interface. The synthesis was carried out in a 50 mL PEEK insert filled with 35 mL solution under hydrothermal conditions at autogenic pressure, and at a temperature of 140–160 °C for 2–96 h. The stainless steel outer shell of the 35 mL autoclave was preheated to the reaction temperature before insertion of the PEEK inserts. After the synthesis time, the autoclave was quenched in water to room temperature. The composite samples were rinsed with demineralized water followed by an ultrasonic treatment (60 Hz, 120 W) for 1 h. Afterwards the samples were dried at 110 °C overnight. Calcination was carried out in an airflow of 50 mL/min with a heating rate of 1 °C/min from 20 to 500 °C followed by a dwell interval for 10 h.

### 2.3. Large scale synthesis of zeolitic coatings

The synthesis mixture was prepared according to the procedure described for the small scale synthesis. The large scale synthesis was carried out in a 3.7 L PEEK insert (ID = 0.2 m) filled with 3 L solution. The temperature of the stainless steel outer shell of the 3 L autoclave was maintained with a 2000 W band heater, which was controlled by a 8200 West controller. During the initial period of 2 h, required to heat up the solution from room temperature to the synthesis temperature, the solution was continuously stirred using a magnetic stirrer to avoid temperature gradients within the autoclave. After this initial period the synthesis proceeded under static conditions as in the 35 mL autoclaves. After the synthesis time, the 3 L autoclave was cooled down to room temperature by circulating cold water through a cooling unit in the stainless steel outer shell. The post-treatment procedure of the composite samples was similar as for the small scale synthesis procedure.

Fig. 1(a) shows a 3D image of the PEEK holder, which was applied in the large scale synthesis procedure. The holder consists of two identical layers referred to as layers A and B, which are the top and bottom layers, respectively. Each layer consists of three symmetrical sets of 12 identical positions, which are indicated in Fig. 1(b). In Table 2 all of the 72 plates are numbered according to their position in the holder.

Table 2
Numbering of the 72 positions for the plates in the holder for the synthesis scale-up procedure

| Layer | Symmetry set | Plate numbers |
|---|---|---|
| A | I | 1–12 |
| | II | 13–24 |
| | III | 25–36 |
| B | I | 37–48 |
| | II | 49–60 |
| | III | 61–72 |

### 2.4. Characterization

The plates were weighted before the synthesis with an analytical mass balance. The weight gain of the plates after the synthesis procedure was used to calculate the zeolite coverage. The Si conversion is defined as:

$$\mathrm{Si}_{\mathrm{conversion}}\ (\%) = \frac{\mathrm{mol}(\mathrm{Si}_{\mathrm{ZSM\text{-}5\ powder}} + \mathrm{Si}_{\mathrm{ZSM\text{-}5\ coating}})}{\mathrm{mol}(\mathrm{Si}_{\mathrm{synthesis\ mixture}})} \times 100 \quad (1)$$

The synthesized coatings were examined by X-ray diffraction (XRD) for phase identification and crystal orientation. XRD data were collected on a Rigaku Geigerflex diffractometer using Cu Kα radiation (1.5405 Å). XRD patterns were recorded in the range of 5–50°, $2\theta$ using step scanning at 0.02°, $2\theta$ per step and a counting time of 4 s for each step. The degree of preferred orientation perpendicular to the *c*-axis of the hexagonal crystals was calculated using the following equation:

$$D_{\mathrm{P2}} = \frac{\text{sums of intensities}(2\,0\,0)\ \text{and}(0\,2\,0)\ \text{XRD peaks}}{\text{intensity of}(0\,0\,2)\ \text{XRD peak}} \quad (2)$$

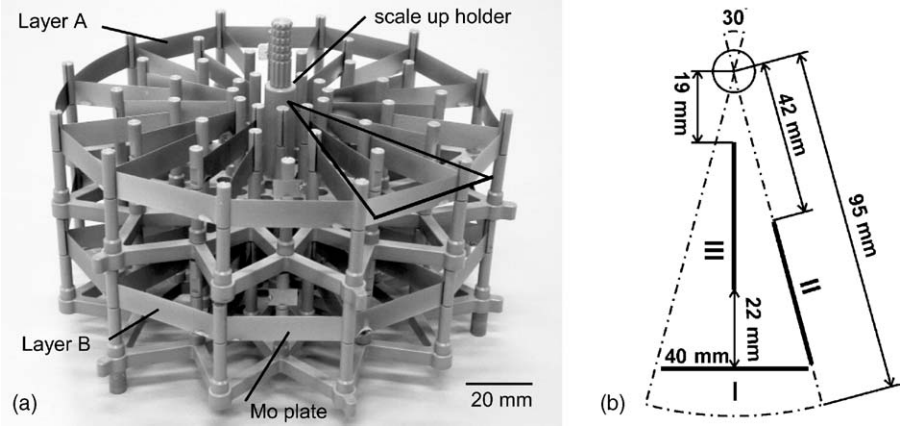


Fig. 1. Holder for the scale-up procedure for zeolite synthesis on 72 plates of 40 × 9.8 × 0.1 mm$^3$: (a) image of the holder consisting of two identical layers (layers A and B), which are positioned on top of each other; (b) schematic top view of the holder geometry (an enlargement of the triangle indicated in (a), 30° of the complete holder is depicted), in which three different symmetry positions of the plates (I, II, and II) are shown. Table 2 summarizes the numbering of the 72 positions for the plates in the holder, which can be divided in six symmetrical sets of 12 plates.

The surface coverage and morphology as well as the layer thickness of the ZSM-5 coatings were examined by SEM on a JEOL JSM-840A.

$N_2$ adsorption isotherms were obtained on an ASAP-2000 Micromeritics instrument with a standard procedure after vacuum pretreatment at 300 °C for 30 h up to a residual pressure <0.1 Pa. The surface area of the zeolitic coating was measured by the BET method at −196 °C in the range of relative pressures within 0.005–0.20, with $N_2$ as the adsorbent. The pore size distribution was obtained with the Horvath–Kawazoe method. The full pore volume was calculated from the maximum adsorption value obtained from the $N_2$ adsorption isotherm. The layer thickness of the coatings ($l$) was calculated, based on measured surface areas ($S$) assuming the BET surface for ZSM-5 crystals ($S_{BET}$) to be 435 $m^2/g$ [21], an apparent density of 0.9 $g/cm^3$ ($d$), and a substrate geometrical area ($A$):

$$l = \frac{S}{AS_{BET}d} \quad (3)$$

Laser scanning confocal microscopy (LSCM) was applied to estimate the layer thickness of the coatings at the intersection between the coated and non-coated parts of the surface. In order to protect a part of the plate from the synthesis mixture, teflon tape was tightly fixed on it. This creates a sharp edge in the zeolitic layer, which was used to determine an average layer thickness from a two-dimensional LSCM height profile.

## 3. Results and discussion

### 3.1. ZSM-5 coating optimization

It was demonstrated that dipping in a template solution just before the synthesis enhances the zeolite growth rate on metal surfaces [19,25]. In case of a multilayer TAMo substrate, the hydrophilicity of an external $TiO_2$ surface and as a result, the zeolite nucleation rate on it, are considerably enhanced by UV pretreatment [26]. The effect of $H_2O$/Si, Si/Al, and TPA/Al ratios on ZSM-5 coverage was investigated after these pretreatments on Mo and TAMo substrates, respectively (Fig. 2). In series A, B, and C the influence of the dilution ratio ($H_2O$/Si) was investigated. Series A was performed on Mo substrates, while series B and C were performed on TAMo substrates at different TPA/Al ratios. Furthermore, series D indicates the effect of the Si/Al ratio on ZSM-5 coverage.

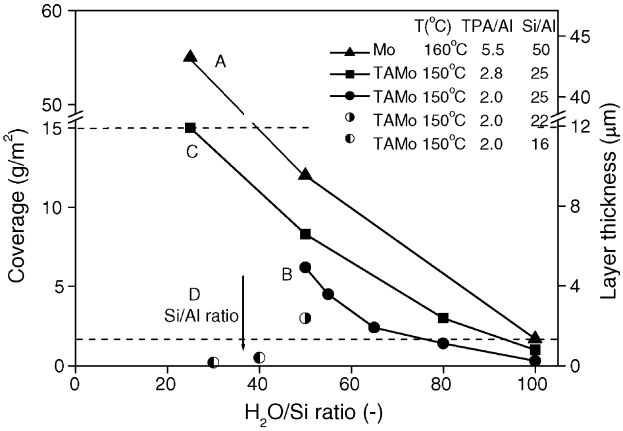


Fig. 2. Effect of the $H_2O$/Si ratio on the ZSM-5 coverage on Mo (series A) and TAMo (series B, C, and D) substrates. Series B and C show the effect of the TPA/Al ratio on the ZSM-5 coverage. The effect of the Si/Al ratio is shown with the arrow pointing down (series D), indicating that lower coverages are obtained at lower Si/Al values. The dashed horizontal lines represent the upper and lower limits of the ZSM-5 coverage.

Fig. 2 shows that the dilution ratio has the largest influence on the zeolite coverage. Therefore, this parameter was optimized first, while other parameters being the same, unless otherwise stated. When the $H_2O$/Si ratio is increased from 24 to 100, a major decrease in ZSM-5 coating thickness was observed from about 45 μm to a single crystal layer. Figs. 3 and 4 shows SEM images of ZSM-5 coatings obtained on Mo (series A) and TAMo (series B) substrates, respectively. At a $H_2O$/Si ratio of 25 and a reaction temperature of 160 °C, a continuous ZSM-5 coating with an average layer thickness of about 45 μm was obtained on a Mo surface. The non-uniform morphology of the coating and the absence of developed crystal faces indicate fast ZSM-5 growth (Fig. 3(a)). High nucleation and crystallization rates are achieved when high super saturations are used. This results in a large number of small, irregularly shaped crystallites showing roughened growth [3]. At higher dilution ratios a more controlled growth of ZSM-5 crystals is obtained. The crystals are oriented parallel to the Mo surface (Fig. 3(c)). The average sizes of the ZSM-5 crystals in the direction of the crystallographic axes $a$, $b$, and $c$ are 7, 2, and 11 μm, respectively. The relatively large crystals with well-developed crystal faces cause discontinuity in the oriented crystal layer [3]. Pinholes in the ZSM-5 coatings are observed in Fig. 3(b and c).

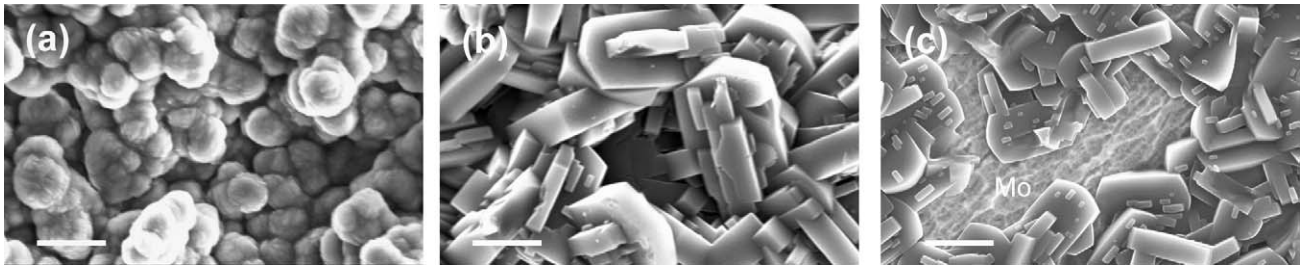


Fig. 3. Scanning electron micrographs of ZSM-5 coatings at different dilution ratios on a Mo substrate (series A of Fig. 2). Conditions: 160 °C, 48 h, Si/Al = 50, TPA/Al = 5.5 at $H_2O$/Si ratios of (a) 25, (b) 50, and (c) 100. Scale bar indicates 10 μm.

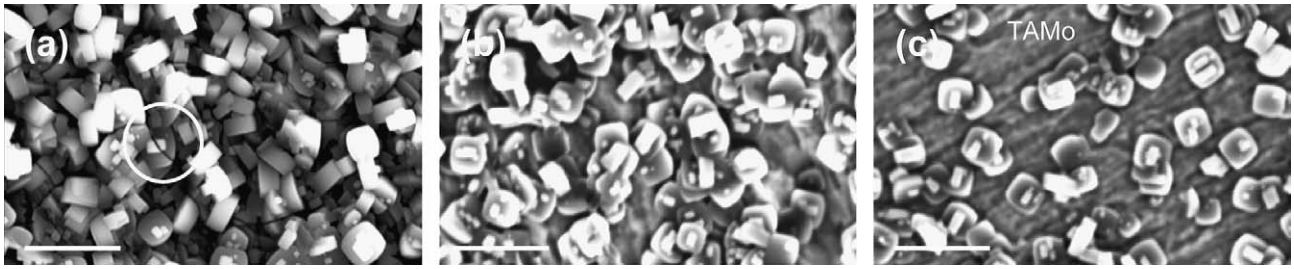


Fig. 4. Scanning electron micrographs of ZSM-5 coatings at different dilution ratios on a TAMo substrate (series B of Fig. 2). Conditions: 150 °C, 48 h, Si/Al = 25, TPA/Al = 2.0 at $H_2O$/Si ratios of (a) 50, crack in the ZSM-5 crystals indicates the coating stability (circle), (b) 65, and (c) 100. Scale bar indicates 10 μm.

For catalytic applications, the presence of framework Al can be essential, since it determines the acidity as well as the ion-exchange ability of the zeolite. The decrease in the Si/Al ratio from 50 to 25 decreased the average size of the ZSM-5 crystals to $3.5 \times 1 \times 4$ $\mu m^3$ in the direction of the crystallographic axes *a*, *b*, and c, respectively (Fig. 4). This is in line with earlier reported data that aluminium rich crystals are smaller in size than the more siliceous ones [20]. The $H_2O$/Si ratio has no profound effect on the crystal sizes on the TAMo substrate, which is in contrast to a study performed on a stainless steel substrate [22]. The ZSM-5 crystals preferentially grow on crystals already connected to the surface (Fig. 4(c)), although there are still uncovered areas on the TAMo surface. This suggests that the growth process under these conditions is determined by diffusion of the reactants to and not by formation of the zeolite crystals [20]. Oudshoorn reported relatively low activation energies for nucleation and for crystal growth, which are characteristic for diffusional limited systems. Nevertheless, a uniform ZSM-5 coating was obtained on the TAMo substrate at a $H_2O$/Si ratio of 50. Ten similar experiments confirmed a good synthesis reproducibility producing a coverage of $6.2 \pm 0.5$ g/m$^2$. Several cracks in the coatings were seen after calcination (Fig. 4(a)), which indicates a strong chemical attachment of the coating to the surface of the TAMo substrate. Further decreasing of the Si/Al ratio resulted in a considerable decrease both in coverage (series D of Fig. 2) and in crystal size. Although still a substantial coverage was obtained at a Si/Al value of 22, the lower value of 16 reduced the ZSM-5 coverage below 0.5 g/m$^2$.

The template concentration determines the pH of the synthesis mixture and therefore the zeolite nucleation and crystallization kinetics, which increases at higher pH. However, too fast crystallization leads to low crystallinity. Furthermore, dissolution of the support has to be prevented during the time needed to form a crystalline phase [3]. Therefore, the TPA/Al ratio was also optimized. When a TPA/Al ratio of 5.5 was applied on the TAMo substrate, especially at a low surface roughness, the $TiO_2$ partly dissolved as a result of the high pH of 13.5. At lower TPA/Al values of 2.8 and 2.0 (series B and C in Fig. 2), no dissolution of the $TiO_2$ layer was observed, and ZSM-5 crystals were successfully grown on the TAMo surface. At the higher template concentration (series C), higher coverages were obtained and small crystals were formed. The average crystal volume is reduced from about 15 to 3 $\mu m^3$ when the TPA/Al ratio is increased from 2 to 2.8.

Fig. 5(a and b) shows typical XRD patterns of as-synthesized ZSM-5 coatings on a TAMo substrate. All peak locations correspond to the ZSM-5 reference in Fig. 5(e) [27]. The XRD pattern of a calcined ZSM-5 coating on a TAMo substrate is shown in Fig. 5(c). Removal of the template from the zeolitic coatings occurs at 350–500 °C and is accompanied by a substantial shrinkage in the zeolite framework [28]. The *a*-, *b*-, and *c*-axis contraction is non-uniform in MFI zeolite crystals, which changes the relative intensities of the diffraction peaks as can be seen in Fig. 5(c). $MoO_3$ peaks were not observed, which proofs the stability of the ZSM-5 coating and the protective effect of the $Al_2O_3$ layer. However, Mo-oxides (especially $MoO_3$ phase) were identified by XRD after calcination of ZSM-5 coatings on regular Mo substrates. The oxide layer on the Mo surface deteriorates the coating stability, which eventually causes delamination of the zeolitic layer.

The XRD patterns of the zeolitic coatings are consistent with the ZSM-5 structure, however, the relative peak intensities are different from those of zeolite powders. Strong peaks are observed at $2\theta$ of 7.49, 8.80, 8.90, 23.10, and 23.98°, corresponding to diffraction of (0 1 1), (0 2 0), (2 0 0), (0 5 1), and (0 3 3), respectively [27]. Values of $D_{P2}$ were

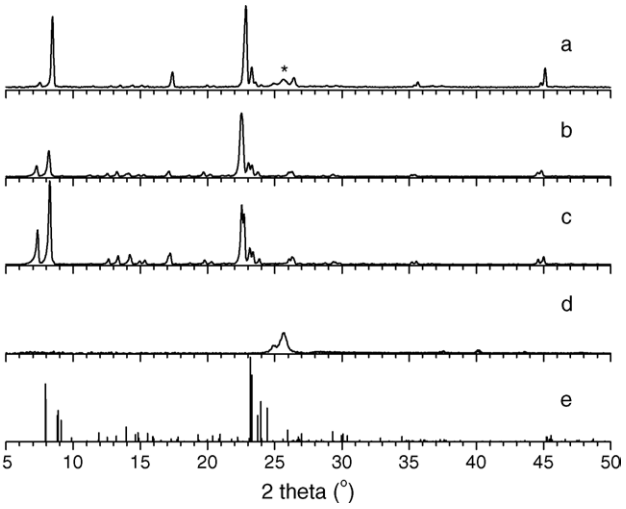


Fig. 5. XRD patterns: (a) as-synthesized coating on TAMo substrate of series B, $H_2O$/Si = 65, (b) as-synthesized coating obtained after scale-up experiment (experiment L2 of Table 3), (c) calcined coating obtained after scale-up experiment (experiment L2 of Table 3), (d) TAMo substrate, and (e) reference for tetrapropylammonium ZSM-5 [27]. Asterisk in (a) depicts the reflection given by the TAMo substrate (d).

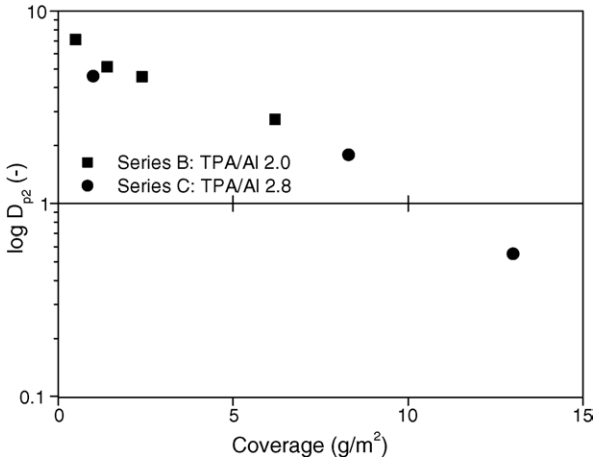


Fig. 6. Orientation of ZSM-5 crystals ($D_{P2}$) on a TAMo substrate for series B and C (Fig. 2). $D_{P2}$ values indicate the preferred alignment perpendicular to the *c*-axis. The horizontal line at a $D_{P2}$ value of 1 represents a random orientation of powder ZSM-5 crystals (calculated from [27]).

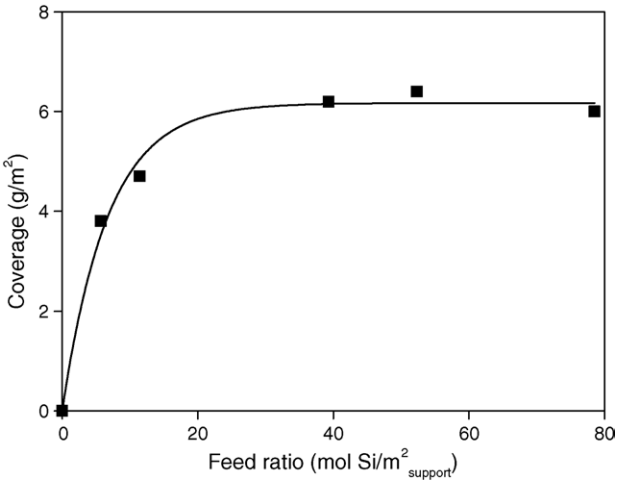


Fig. 7. Effect of the feed ratio on ZSM-5 coverage. Conditions: 150 °C, 48 h, Si/Al = 25, TPA/Al = 2.0, and $H_2O$/Si = 50.

calculated for the ZSM-coatings of series B and C (Fig. 2). Fig. 6 shows the dependence of the $D_{P2}$ values on the zeolite coverage. The relatively high values of $D_{P2}$ at a low ZSM-5 coverage, corresponding to a coating thickness of less than one single crystal layer, reveal a more profound alignment with the *c*-axis parallel to the substrate surface. At a higher coverage, the preferred orientation disappears when $D_{P2}$ values reduce to unity. In ZSM-5 coatings with a thickness larger than 2 μm most of the crystalline material has adapted an orientation with both the *a* and *b* axes pointing away (but not perpendicular to) from the substrate surface [29]. In thin ZSM-5 films, the crystals are preferentially oriented with the *a*-axis (sinusoidal channels) or the *b*-axis (straight channels) perpendicular to the substrate surface [19,30]. Orientation is caused by the preferential growth of the *ac*-plane of the crystallites in the plane of the substrate surface [31].

The ZSM-5 coverage is a function of the feed-to-support area ratio (mol $Si/m^2_{support}$) [20,21]. The influence of this ratio was investigated by varying the amount of support, that is the total surface area of the support, while keeping the amount of synthesis mixture the same. Fig. 7 shows that the coverage on the TAMo substrate is independent of the feed-to-support area ratio at values above 30 mol $Si/m^2_{support}$ for the specific synthesis conditions. Based on this value it was decided to fix the volume of the autoclave at 3 L for the scale-up synthesis, which resulted in a feed-to-support area ratio of 47 mol $Si/m^2_{support}$.

### 3.2. Scale-up of in situ synthesis

The main goal of the scale-up procedure is to obtain the same and uniform ZSM-5 coverage on all plates of $40.0 \times 9.8 \times 0.1$ mm$^3$. A dedicated plate holder for 72 plates was designed to maximize the distance between the plates, within a total volume of 3 L (Fig. 1). The open structure of the holder provides equal accessibility of the nutrients to the substrate surfaces during the crystallization process. The reaction conditions as well as the synthesis mixture composition have to be chosen such that neither heat nor mass transfer limitations will be present in the synthesis volume. The synthesis conditions were optimized at a $H_2O$/Si ratio of 50 to provide a feed-to-support area ratio of 47 mol $Si/m^2_{support}$. This ratio gives a Si conversion below 50%, which will ensure that the synthesis mixture will not be locally depleted, preventing concentration gradients. The effect of the different heating rates in the 35 mL and 3 L autoclaves as well as the effect of stirring was investigated (Table 3).

The effect of the different heating rates on the ZSM-5 coverage was examined in experiments S1 and L1. The temperature of the synthesis mixture in the 3 L autoclave approaches the set-point much faster due to direct contact of the autoclave with a heating cartridge, while the 35 mL autoclave is heated by a convection oven (Fig. 8). As a result the temperature of the synthesis mixtures in the 35 mL and 3 L autoclaves reached the set-point with different average rates of

Table 3
Synthesis scale-up procedure: effect of initial heating-up period and stirring[a]

| Run number[b] | $T_{rate}$ (°C/min) | Stirring | Coverage (g/m$^2$) | | | | | | Si conversion (%) | BET (m$^2$/g) |
|---|---|---|---|---|---|---|---|---|---|---|
| | | | Set | | | | | | | |
| | | | AI | AII | AIII | BI | BII | BIII | | |
| S1 | 0.6 | No | 6.2 | | | | | | 40 | 410 |
| L1 | 1.3 | No | – | – | – | 9.1 | 8.9 | 8.6 | 33 | |
| L2 | 1.3 | Yes | 14.79 | 14.66 | 14.54 | 14.87 | 14.82 | 15.16 | 33 | 370 |

[a] Synthesis condition in all experiments; $50SiO_2$:$1Al_2O_3$:4TPAOH:$2500H_2O$, at 150 °C, 48 h.
[b] S denotes 35 mL autoclave; L denotes 3 L autoclave.

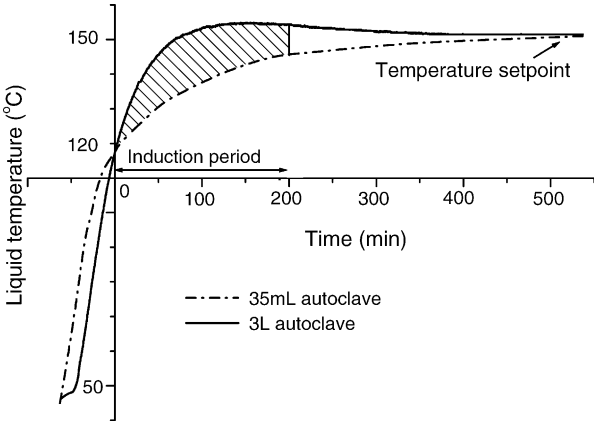


Fig. 8. Liquid temperature as a function of time during heating up of the 35 mL and 3 L autoclaves. The shaded area indicates the estimated induction period, in which the liquid temperature of the 3 L autoclave is higher than that of the 35 mL autoclave.

0.6 and 1.3 °C/min, respectively. When a similar batch composition was used for the synthesis, coverages of 6.2 and 8.9 g/m$^2$, and a Si conversion of 40 and 33%, were obtained in the 35 mL and 3 L autoclaves, respectively (Table 3). These results can be attributed to the higher heating rate in the 3 L autoclave.

The primary event during the temperature raise of the reaction mixture from the aging to the synthesis temperature, that is from 47 to 150 °C, is the accelerated dissolution of the (alumino)silicate gel phase, resulting in higher concentration and mobility of monomeric silicate and aluminate species [32]. Zeolite crystallization is expected after an induction period in which nucleation occurs. Nucleation of Si-TPA-ZSM-5 particles from clear solutions occurs via association of secondary amorphous particles and monomeric silicate in a TPA mediated synthesis [33,34]. When the solubility of the amorphous particles increases, the presence of secondary particles decreases, which results in a reduced nucleation rate. Since the total amount of ZSM-5 crystals formed during the synthesis experiment is dependent on the nucleation rate, zeolite formation in the bulk was considerably reduced as the Si conversion decreased from 40 to 33%.

The higher temperature increase of the 3 L autoclave resulted in an increased ZSM-5 coverage on the support. Koegler et al. proposed a Si-ZSM-5 thin film growth model on a support [31]. At the start of the synthesis the silica gel is deposited on the support, forming a thin, low-density silica surface. At a stage where the gel layer formation is reduced, nucleation will occur at the interface of the gel and the synthesis solution, where the template and silica source are present in abundance. The rate of nucleation is dependent on the availability of soluble silicate. The use of a monomeric silica source as TEOS and the presence of sodium in the synthesis mixture [34] as well as an elevated reaction temperature facilitates the dissolution of a condensed silica precursor. Nucleation and crystallization of ZSM-5 crystals on stainless steel already occurs at 110 °C [20]. In the synthesis of Si-TPA-MFI at 125 °C a nucleation period of approximately 200 min was reported [35,36]. The shaded area in Fig. 8 indicates the period in which the liquid temperature in the 3 L autoclave is higher than in the 35 mL autoclave yielding a higher nucleation

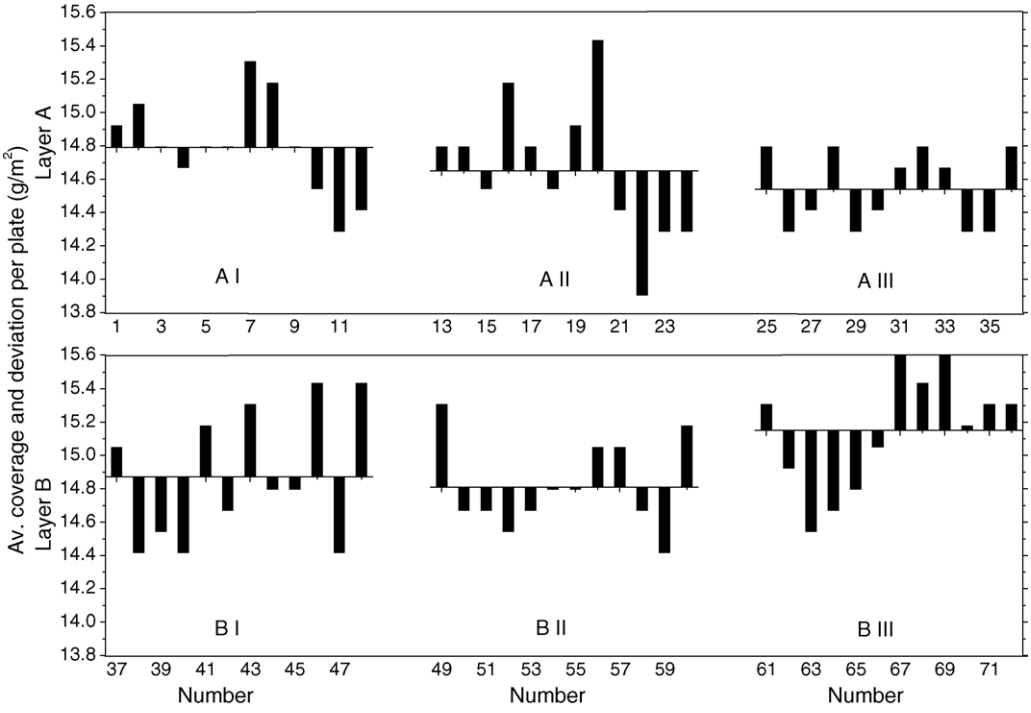


Fig. 9. ZSM-5 coverage on the 72 TAMo substrates after the scale-up procedure. The average coverage per symmetry set is given for both layers A and B as well as the deviation per individual plate. Conditions: 150 °C, 48 h, Si/Al = 25, TPA/Al = 2.0, $H_2O$/Si = 50, and a feed ratio of 47.5 mol Si/$m^2_{support}$ (3 L of synthesis mixture). The synthesis mixture was stirred during the initial 2 h of the heating up period.

rate on the corresponding substrates. Similar findings were reported for the in situ synthesis of zeolite A on stainless steel. When the substrate was directly heated, zeolite nucleation and crystallization in the bulk was suppressed and promoted that on the substrate [37].

Experiment L1 resulted in a relatively large variation in coverage between different symmetrical positions in the holder. The coverage decreased from 9.1 to 8.6 g/m$^2$ for plates positioned near the wall of the PEEK inserts to plates positioned in the centre of the synthesis mixture. The difference between symmetry sets I, II, and III can be attributed to the initial temperature of the synthesis mixture, being higher near the wall of the insert. This initial temperature gradient in the synthesis volume during the heating period can be avoided by stirring of the mixture.

The effect of stirring during the heating period was investigated in experiment L2. The average coverage and the total deviation per plate for all six symmetrical sets of the holder are depicted in Fig. 9. The average ZSM-5 coverage is 14.8 g/m$^2$ and the standard deviation over all 72 plates is $\pm$0.4 g/m$^2$. The average coverage of the substrates of all six symmetrical sets of plates is within this range (experiment L2 of Table 3). The relatively small and non-systematic differences between the separate sets prove that no axial nor radial concentration gradients were present in the synthesis volume during the zeolite synthesis procedure in the 3 L autoclave. Furthermore, one may conclude that the formation of crystallites, formed in the homogeneous bulk phase, and the effect of gravity play no role in the scale-up synthesis procedure, when the Si conversion is below 50%. Fig. 5(b and c) shows the XRD patterns of the as-synthesized and the calcined ZSM-5 coatings obtained in the scale-up procedure. The coverage on the TAMo substrates after the scale-up experiment L2 is about 1.7 times higher than that obtained in the scale-up experiment L1, in which no stirring was applied. This difference can be explained by the effect of stirring during the initial heating up period. The ZSM-5 growth on the substrate surface, that is the coating selectivity, was greatly enhanced as a result of the initial stirring of the liquid. Stirring of the liquid increases the chance that nuclei or crystals formed in the homogeneous liquid phase, away from the support surface, collide with, or are carried onto, the support surface or the zeolitic coating that has already formed on the surface. A doubling of coating selectivity was reported for in situ synthesis of ZSM-5 on stainless steel monoliths in case of stirring of the synthesis mixture [25].

## 4. Conclusions

ZSM-5 coatings with a wide range of Si/Al ratios between 16 and 50 have been prepared on Mo and surface modified $TiO_2/Al_2O_3$/Mo substrates by hydrothermal synthesis. The effect of the synthesis mixture composition on ZSM-5 coverage was investigated. The thickness of the coatings can be adjusted from a single crystal layer to a multi layer with a thickness of 45 μm by applying different $H_2O$/Si ratios.

A scale-up procedure has been developed for hydrothermal synthesis of uniform ZSM-5 coatings on a set of 72 molybdenum plates of 40 × 9.8 × 0.1 mm$^3$ in a 3 L autoclave. A coverage of 14.8 ± 0.4 g/m$^2$ was obtained on all plates in the scale-up procedure. The deviation in coverage on the separate plates did not exceed 3%.

In the scale-up procedure, the positive effect of the fast heating of the synthesis mixture on the enhancement of zeolite coverage was demonstrated. At higher temperatures, the solubility of chemicals in the mixture increases, which decreases the nucleation rate in the bulk volume of the autoclave, while the ZSM-5 growth at the surface of the substrate is enhanced. The ZSM-5 coverage can be increased further by stirring of the synthesis mixture. Stirring of the liquid increases the opportunity that nuclei or crystals, formed in the bulk liquid, collide with, or are carried onto, the plate surface or the zeolitic coating.

## Acknowledgements

The financial support by the Dutch Technology Foundation (STW, project no. EPC.5543), Shell International Chemicals B.V., Akzo Nobel Chemicals B.V., and Avantium Technologies B.V. are gratefully acknowledged. The authors would also like to thank Dr. Milja Mäkelä from Nanoscale Oy (Finland) for her co-operation in the optimization of the ALD procedure.

## References

[1] J. Caro, M. Noack, P. Kölsch, R. Schäfer, Micropor. Mesopor. Mater. 38 (2000) 3.
[2] L. Scandella, G. Binder, T. Mezzacasa, J. Gobrecht, T. Berger, H.P. Lang, Ch. Gerber, J.K. Gimzewski, J.H. Koegler, J.C. Jansen, Micropor. Mesopor. Mater. 21 (1998) 403.
[3] J.C. Jansen, J.H. Koegler, H. van Bekkum, H.P.A. Calis, C.M. van den Bleek, F. Kapteijn, J.A. Moulijn, E.R. Geus, N. Van der Puil, Micropor. Mesopor. Mater. 21 (1998) 213.
[4] H.P. Calis, A.W. Gerritsen, C.M. van den Bleek, C.H. Legein, J.C. Jansen, H. van Bekkum, Can. J. Chem. Eng. 73 (1995) 120.
[5] G.B.F. Seijger, O.L. Oudshoorn, A. Boekhorst, H. van Bekkum, C.M. van den Bleek, H.P.A. Calis, Chem. Eng. Sci. 56 (2001) 849.
[6] Wa̧claw, K. Nowińska, W. Schwieger, Appl. Catal. A: Gen. 270 (2004) 151.
[7] T. Osawa, I. Nakano, O. Takyasu, Catal. Lett. 86 (2003) 57.
[8] Y. Li, J.N. Armor, J. Catal. 173 (1998) 511.
[9] Y. Li, J.N. Armor, J. Catal. 176 (1998) 495.
[10] G. Kolb, V. Hessel, Chem. Eng. J. 98 (2004) 1.
[11] M.J.M. Mies, E.V. Rebrov, M.H.J.M. de Croon, J.C. Schouten, Chem. Eng. J. 101 (2004) 225.
[12] A. Gavriilidis, P. Angeli, E. Cao, K. Yeong, Y.S.S. Wan, Trans. IChem Eng. 80 (2002) 3.
[13] P. Pfeifer, A. Wenka, K. Schubert, M.A. Liauw, G. Emig, AIChE J. 50 (2) (2004) 418.
[14] E.R. Delsman, M.H.J.M. de Croon, G.D. Elzinga, P.D. Cobden, G.J. Kramer, J.C. Schouten, Chem. Eng. Technol. 28 (3) (2005) 1.
[15] J. Coronas, J. Santamaria, Chem. Eng. Sci. 59 (2004) 4879.
[16] S.P. Davis, E.V.R. Borgstedt, S.L. Suib, Chem. Mater. 2 (1990) 712.
[17] J.C. Jansen, W. Nugroho, H. van Bekkum, in: R. Von Ballmoos, J.B. Higgins, M.M.J. Treacy (Eds.), Proceedings of the 9th International Zeolite Conference, Montreal, 5–10 July, 1992), p. 247.
[18] V. Valtchev, S. Mintova, Zeolites 15 (1995) 171.
[19] R.K. Grasselli, R.M. Lago, R.F. Socha, J.G. Tsikoyiannis, US patent 5349117, 1994.
[20] O.L. Oudshoorn, Zeolitic coatings applied in structured catalyst packings, Ph.D. Thesis, Delft University of Technology, 1998.

[21] G.B.F. Seijger, O.L. Oudshoorn, W.E.J. van Kooten, J.C. Jansen, H. van Bekkum, C.M. van den Bleek, H.P.A. Calis, Micropor. Mesopor. Mater. 39 (2000) 195.
[22] E.V. Rebrov, G.B.F. Seijger, H.P.A. Calis, M.H.J.M. de Croon, C.M. van den Bleek, J.C. Schouten, Appl. Catal. A: Gen. 181 (2001) 355.
[23] S.A. Kuznetsov, S.V. Kuznetsova, E.V. Rebrov, M.J.M. Mies, M.H.J.M. de Croon, J.C. Schouten, Surf. Coat. Technol., in press.
[24] J.C. Schouten, E.V. Rebrov, M.H.J.M. de Croon, Chimia 56 (2002) 627.
[25] Z. Shan, W.E.J. van Kooten, O.L. Oudshoorn, J.C. Jansen, H. van Bekkum, C.M. van den Bleek, H.P.A. Calis, Micropor. Mesopor. Mater. 34 (2000) 81.
[26] A.W.C. van den Berg, L. Gora, J.C. Jansen, T. Maschmeyer, Micropor. Mesopor. Mater. 66 (2003) 303.
[27] H. van Koningsveld, H. van Bekkum, J.C. Jansen, Acta Crystallogr. B43 (1987) 127.
[28] J. Dong, Y.S. Lin, M.Z.-C. Hu, R.A. Peascoe, E.A. Payzant, Micropor. Mesopor. Mater. 34 (2000) 241.
[29] J. Hedlund, O. Öhrman, V. Msimang, E. van Steen, W. Böhringer, S. Sibya, K. Möller, Chem. Eng. Sci. 59 (2004) 2647.
[30] J. Hedlund, S. Mintova, J. Sterte, Micropor. Mesopor. Mater. 28 (1999) 185.
[31] J.H. Koegler, H. van Bekkum, J.C. Jansen, Zeolites 19 (1997) 262.
[32] J.C. Jansen, Introduction to zeolite science and practice, in: H. van Bekkum, E.M. Flanigen, P.A. Jacobs, J.C. Jansen (Eds.),2nd ed., Studies in Surface Science and Catalysis, vol. 137, Elsevier, Amsterdam, 2001, , p. 196Chap. 5A,.
[33] S.L. Burkett, M.E. Davis, Chem. Mater. 7 (1995) 920.
[34] S.L. Burkett, M.E. Davis, Chem. Mater. 7 (1995) 1453.
[35] P.P. de Moor, The mechanism of organic-mediated zeolite crystallization, Ph.D. Thesis, Eindhoven University of Technology, 1998.
[36] K.A. Carlsson, J. Warzywoda, A. Sacco Jr., Zeolites and mesoporous materials at the dawn of the 21st century, in: A. Galarneau, F. Di Renzo, F. Fajula, J. Vedrine (Eds.), Studies in Surface Science and Catalysis, vol. 135, Elsevier, Amsterdam, 2001, p. 188.
[37] A. Erdem-Şenatalar, M. Tatlier, M. Ürgen, Micropor. Mesopor. Mater. 32 (1999) 331.